Published in final edited form as:
J Neurosurg. 2010 March ; 112(3): 479–490. doi:10.3171/2009.6.JNS081161.

Subthalamic nucleus deep brain stimulator placement using high-field interventional magnetic resonance imaging and a skull-mounted aiming device: technique and application accuracy

Philip A. Starr, M.D., Ph.D.[1], **Alastair J. Martin, Ph.D.**[2], **Jill L. Ostrem, M.D.**[3], **Pekka Talke, M.D.**[4], **Nadja Levesque, R.N.**[5], and **Paul S. Larson, M.D.**[1]

[1] Department of Neurosurgery, University of California, San Francisco, California

[2] Department of Radiology, University of California, San Francisco, California

[3] Department of Neurology, University of California, San Francisco, California

[4] Department of Anesthesia, University of California, San Francisco, California

[5] Department of Nursing, University of California, San Francisco, California

Abstract

Object—The authors discuss their method for placement of deep brain stimulation (DBS) electrodes using interventional MR (iMR) imaging and report on the accuracy of the technique, its initial clinical efficacy, and associated complications in a consecutive series of subthalamic nucleus (STN) DBS implants to treat Parkinson disease (PD).

Methods—A skull-mounted aiming device (Medtronic NexFrame) was used in conjunction with real-time MR imaging (Philips Intera 1.5T). Preoperative imaging, DBS implantation, and postimplantation MR imaging were integrated into a single procedure performed with the patient in a state of general anesthesia. Accuracy of implantation was assessed using 2 types of measurements: the "radial error," defined as the scalar distance between the location of the intended target and the actual location of the guidance sheath in the axial plane 4 mm inferior to the commissures, and the "tip error," defined as the vector distance between the expected anterior commissure–posterior commissure (AC-PC) coordinates of the permanent DBS lead tip and the actual AC-PC coordinates of the lead tip. Clinical outcome was assessed using the Unified Parkinson's Disease Rating Scale part III (UPDRS III), in the off-medication state.

Results—Twenty-nine patients with PD underwent iMR imaging–guided placement of 53 DBS electrodes into the STN. The mean (± SD) radial error was 1.2 ± 0.65 mm, and the mean absolute tip error was 2.2 ± 0.92 mm. The tip error was significantly smaller than for STN DBS electrodes implanted using traditional frame-based stereotaxy (3.1 ± 1.41 mm). Eighty-seven percent of leads were placed with a single brain penetration. No hematomas were visible on MR images. Two

Address correspondence to: Philip A. Starr, M.D., Ph.D., Department of Neurosurgery, 533 Parnassus Avenue, Box 0445, San Francisco, California 94143. starrp@neurosurg.ucsf.edu.

Parts of this work were presented in abstract form at the American Association of Neurological Surgeons, Chicago, Illinois, 2008.

Disclosure

This work was supported by research grants from Medtronic, Inc. (2004–2006), and SurgiVision, Inc. (2007–2008), to Drs. Starr, Larson, Martin, and Ostrem. The following authors have also received honoraria for speaking engagements from Medtronic, Inc: Philip A. Starr, Paul S. Larson, and Jill L. Ostrem.

device infections occurred early in the series. In bilaterally implanted patients, the mean improvement on the UPDRS III at 9 months postimplantation was 60%.

Conclusions—The authors' technical approach to placement of DBS electrodes adapts the procedure to a standard configuration 1.5-T diagnostic MR imaging scanner in a radiology suite. This method simplifies DBS implantation by eliminating the use of the traditional stereotactic frame and the subsequent requirement for registration of the brain in stereotactic space and the need for physiological recording and patient cooperation. This method has improved accuracy compared with that of anatomical guidance using standard frame-based stereotaxy in conjunction with preoperative MR imaging.

Keywords

deep brain stimulation; interventional MR imaging; surgical methods; neurosurgery; subthalamic nucleus; Parkinson disease

---

Deep brain stimulation is a widely used technique for reversible modulation of subcortical brain function. There have been 2 predominant technical approaches to placing DBS devices: frame-based stereotaxy and frameless neuronavigation–guided implantation using a skull-mounted aiming device, in conjunction with bone-implanted fiducial markers. In both techniques, brain images used for targeting (CT and/or MR imaging) are obtained preoperatively. Surgical planning software is used to register brain targets in an image space ("stereotactic space") defined by the frame geometry or by bone-implanted fiducial markers. Placement of the DBS lead subsequently takes place in a standard operating room by navigation in stereotactic space, which is assumed to remain immobile with respect to the brain target. The application accuracies of these techniques have been measured both with phantoms[11,18] and in human patients undergoing DBS implantation.[12] Frequently, the initial anatomical target is refined by intraoperative MER to improve the final lead placement. This adds time, invasiveness, and complexity to the procedure.

Interventional MR imaging is a technique in which real-time MR imaging guidance is used for invasive procedures; this technique has recently been applied to tumor resection[5,13,14] and brain biopsy sampling.[9,21] We have previously reported on phantom testing, and early clinical experience (with 8 lead implants) with iMR imaging– guided implantation of DBS electrodes into the STN for PD.[19] Our approach uses a standard configuration (closed bore) 1.5-T MR imaging unit located in a radiology suite rather than an intraoperative MR imager specifically configured for neurosurgery. The key features of this approach are: 1) planning, insertion, and MR imaging confirmation of DBS lead placement are integrated into a single procedure while the patient is on the MR gantry; 2) the platform for inserting the DBS lead is a bur hole–mounted trajectory guide rather than a traditional stereotactic frame and arc system; 3) target coordinates are defined with respect to the MR imaging isocenter rather than to a separate stereotactic space using fiducial markers; 4) patients are positioned supine in a state of general anesthesia and no MER or test stimulations are performed; and 5) target images are acquired after bur hole creation and intracranial air entry, reducing the potential for errors associated with brain shift that can occur when conventional techniques are used in between image acquisition and probe insertion.

In the present study we report the technique and application accuracy for iMR imaging–guided placement of 53 DBS electrodes into the STN in 29 patients with PD, and show the statistical superiority of the accuracy of this method over STN DBS with frame-based stereotaxy.

Methods

Patient Population

All patients had idiopathic PD, diagnosed by a neurologist specializing in movement disorders (J.L.O.), and met the standard criteria for STN DBS as described elsewhere. [15] For patients who underwent bilateral electrode implantation, scores on the UPDRS part III were obtained at baseline and at 6–12 months after implantation. The study was approved by the University of California, San Francisco, institutional review board, and written informed consent was obtained from each patient.

Interventional MR Imaging–Guided Implantation

The technical approach has been described previously in the initial 8 implantations,[19] but is detailed here to include more recent refinements introduced as the method has evolved. The specialized devices and MRcompatible equipment used are listed in Table 1, and MR protocols are shown in Table 2. The guidance platform used was the the NexFrame DBA (deep brain access) trajectory guide. This is a single-use item that mounts over a bur hole with 3 bone screws. The device is aimed at a target using a rotate/translate mechanism, maintaining a constant pivot point. The NexFrame can accept 2 possible inserts: an MR-visible alignment stem, or a “multi-lumen insert” containing 5 parallel channels (3-mm separation) for guiding probes into the brain. The basic NexFrame platform is identical to that used for frameless neuronavigation –guided DBS,[12] but the 2 inserts are specialized for the interventional MR imaging application.

Patient Preparation and Positioning

Patients were allowed to take their usual morning dose of antiparkinsonian medications. After premedication with midazolam and fentanyl, general anesthesia was induced with propofol in a room adjacent to the MR imaging suite. Anesthesia was maintained with sevoflurane and intermittent fentanyl and vecuronium boluses. Ventilation was adjusted to maintain end-tidal CO_2 between 35 and 40 mm Hg. After placement of a radial artery catheter, the patients’ heads were placed into a carbon fiber headholder designed to mount directly onto the MR imaging gantry. The frontal area was shaved using clippers. An array of 4 flexible surface coils positioned at the sides, top, back, and front of the head was used for MR signal reception (Fig. 1).

Trajectory Planning for Bur Hole Location

Patients were then moved into the bore of the MR imager. An MR imaging–compatible anesthesia machine was used. A landmark was established on the frontal scalp near the presumed coronal suture and advanced to magnet isocenter. A Gd-enhanced volumetric gradient echo MR imaging was obtained (scan parameters in Table 2, MR protocol 1) parallel to the line between the AC and PC. On the MR console, approximate anatomical targets were selected bilaterally at a point 12 mm lateral, 3 mm posterior, and 4 mm inferior to the midcommissural point. These targets were used only for trajectory planning, however, because final anatomical target selection was performed in a subsequent step (described below). Single-slice, oblique, parasagittal reformatted images were reconstructed that passed through the approximate targets, but avoided the lateral ventricle. A trajectory that avoided sulci and cortical veins was then selected on the oblique image (Fig. 2). At the point where the trajectory crossed the scalp, a rapidly updating MR fluoroscopy sequence (MR protocol 2, described further below) was prescribed with its center at the intended entry point. The surgeon reached into the bore of the magnet and manually placed an MR-visible pointer at the intended entry point. This was marked with a pen, the patient was moved to the back of

the bore, and the skull marked percutaneously by injecting methylene blue through a 22-gauge needle at the scalp entry site.

Initial Exposure and Mounting of Trajectory Guide

The frontal area was prepared and draped with a bore drape designed to keep the surgical field sterile yet tolerate head movement between the center and back of the bore (a distance of ~ 1 m) (Fig. 3A). A pressurized nitrogen tank, electrical power sources for bipolar cautery, one headlight, and one floor light were placed outside the MR imaging room with the regulator hose and electrical cords directed through the waveguide. Monopolar cautery was not used. After making coronally oriented incisions, 14- mm frontal bur holes were drilled with an MR compatible cranial drill. The base rings for the Stimloc lead anchoring device and the NexFrame trajectory guides were mounted over the bur holes. The dura mater was opened bilaterally and the leptomeninges were coagulated. The trajectory guide alignment stems were filled with sterile saline and mounted into the trajectory guides (Fig. 3B).

Target Definition and Aiming of Alignment Stem

Patients were moved to reposition the head at the magnet isocenter. Table movement was then disabled and no further patient movement was allowed until the leads were inserted and placement was confirmed on imaging. High-resolution T2-weighted axial MR images were obtained with 2-mm slice thickness, aligned such that 1 slice passed 4 mm inferior to the commissures (MR protocol 3). The brain target was selected on this image (Fig. 4). The intended target was generally very close to the default coordinates of 12 mm lateral, 3 mm posterior, and 4 mm inferior to the midcommissural point. However, small adjustments in the default coordinates were made based on direct visualization of the borders of the STN and red nucleus, so as to place the target within the dorsolateral STN at least 2 mm from the medial, lateral, and posterior borders. Axial and coronal volumetric T2- weighted MR imaging was performed through the pivot points of the alignment stems (MR protocol 4; Fig. 5). The x, y, and z coordinates of the target and pivot with respect to the MR isocenter were determined by placing a “region of interest” cursor over the desired location. The final x, y, and z coordinates of the pivot were a synthesis of the values on coronal and sagittal views.

For the first side to be implanted, the x, y, and z coordinates of the target and pivot were used to prescribe the MR fluoroscopy sequence (MR protocol 2). The target and pivot points define a line and the MR scan is prescribed such that it is perpendicular to and centered on this trajectory at a location 9–10-cm superior to the bur hole. The surgeon donned a sterile hood to maintain the sterile field, and reached into the bore of the magnet to manually align the stem to the target line, while viewing the MR fluoroscopy image on an in-room monitor. When the desired alignment was achieved, the NexFrame was locked into place. Rapid, low-resolution, oblique coronal and sagittal images (MR protocol 5) were obtained along the orientation of the stem, and the final anticipated target reconstructed graphically (Fig. 6). Occasionally, the oblique scans predicted a trajectory not perfectly aligned with the intended target. In these cases a new alignment scan was prescribed with its center slightly modified, and manual alignment was again performed by the surgeon. The distance from the target to the relevant level of the trajectory guide (the step-off between thick and thin sections of the alignment stem) was measured on oblique images to allow calculation of the position of the depth stop in the subsequent step. The distance was increased by 4.5 mm so that the sheath and stylet would slightly overshoot the target.

Insertion of Guidance Sheath and Lead

The alignment stem was replaced with a 5-channel multilumen insert, and a ceramic stylet within a plastic peel-away sheath was placed into the center lumen (Fig. 3C). A depth stop was placed on the stylet at the appropriate length as described above. The stylet/sheath assembly was advanced into the brain in 2–3 stepwise movements and monitored via inplane MR imaging with oblique sagittal and coronal T2 sequences (MR protocol 6). The alignment and insertion procedure were then repeated for the contralateral side. A high resolution axial T2-weighted image was obtained through the target area to assess sheath/stylet position at the target (MR protocol 3) (Fig. 7).

If placement of the peel-away sheath/stylet assembly was found to be inappropriate for either side (defined as distance between intended and actual stylet position of > 2 mm in the axial plane 4 mm below the commissures), a side channel of the NexFrame multilumen insert was considered to provide a parallel track with an offset of 3 mm in a direction perpendicular to the lead trajectory. If an offset of 3 mm could not provide appropriate placement, the sheath and stylet were removed, alignment stem replaced, and the NexFrame trajectory readjusted by repeating the alignment scans.

Two 28-cm DBS leads (Medtronic model 3389–28), were prepared by replacing their standard wire stylet with custom-made, nonferrous titanium wire stylets (supplied by Medtronic, Inc.) so as to allow imaging of the lead with the wire stylets in place and without excessive artifact. On 1 side, the ceramic stylet within the peelaway sheaths was removed and a “bridge” snapped over the multilumen insert. The bridge provided a space between itself and the multilumen insert for the sides of the peel-away sheath, and contained a lead-holding screw. A depth stop was placed on the lead 42.5 mm higher than the depth stop on the ceramic stylet (to account for the extra height of the bridge and lead holder) and the lead was advanced through the sheath to the target. Lead insertion was repeated on the contralateral side. Axial T2- weighted MR imaging was used to confirm lead depth (MR protocol 7).

Closure, Final Imaging, and Implantable Pulse Generator Placement

Patients were moved to position the head at the back of the bore for easier surgical access. The peel-away sheaths were removed. The DBS leads were anchored to the skull with the Stimloc clips. The titanium wire stylets were removed from the leads, and the Stimloc cranial caps set in place. The NexFrame trajectory guides were removed, and the scalp was closed with sutures. Patients were moved back to isocenter for a final high-resolution volumetric T1-weighted MR imaging session (MR protocol 8), to be used to measure the lead tip location and trajectory (Fig. 8). Patients were awakened, allowed to recover in the postanesthesia care unit, monitored overnight in a stepdown unit, and discharged the day after implantation. Lead extenders and a dual channel pulse generator (Medtronic Kinetra) were placed 1–2 weeks later in the standard operating room.

Measurement of Targeting Errors

Two types of errors were measured. The “radial error” was defined as the scalar distance between the location of the intended target and the actual location of the ceramic stylet in the axial plane 4 mm inferior to the commissures on high resolution axial T2-weighted images. This distance was measured directly on the MR console using the ruler tool. In cases where a second placement of the ceramic stylet was made after the first was advanced to the target and deemed inadequate, the first pass was used to calculate radial error. “Tip error” was defined as the distance between the expected AC-PC coordinates of the lead tip, and the actual AC-PC coordinates. The expected AC-PC coordinates were those of the initial target (at a plane of 4 mm below the commissures), corrected in all dimensions by the planned

overshoot of the lead beyond target (4.5 mm), taking into account the double-oblique lead angulation as measured on the final postoperative MR images in Framelink software. The actual AC-PC coordinates of the lead tip were measured using Framelink software as described previously.[28]

Statistical Analysis and Comparison Data Set

To compare DBS lead placement accuracy measurements between iMR imaging and conventional stereotactic techniques, we used a control data set for 76 STN DBS leads placed using standard frame-based stereotaxy in 44 patients, as we previously described in an earlier study.[28] Comparison of mean lead tip errors was performed with unpaired t-tests. We tested iMR imaging errors for correlation with potential error predictors (case order, patient age, side of surgery, sagittal plane trajectory angle, and coronal plane trajectory angle), using the Pearson correlation coefficient r. Statistical significance was set at $p < 0.05$.

Results

Nineteen patients underwent simultaneous bilateral DBS lead implantation, 5 had bilateral implantation staged into 2 separate procedures, and 5 had unilateral implantation only. The mean age ± SD of the patients was 58 ± 8.1 years. The mean surgical time (from initial scalp incision to scalp closure) for simultaneous bilateral implants was 225 ± 30 minutes, and 217 ± 62 minutes for unilateral implantation.

Brain Penetrations

In 46 implantations (87%) only a single brain penetration with the peel-away guidance sheath was necessary to place the lead at the final location. In 4 implantations (8%), the first placement of the stylet/sheath, at target depth, was considered inaccurate based on a > 2-mm radial error (measured in the plane 4 mm below the commissures). In these cases, the sheath and stylet were withdrawn completely and replaced either through a parallel port of the multilumen insert (in 3 cases), or by replacing the alignment stem into the NexFrame and performing a new target alignment (in 1 case). In another 3 implantations, the sheath/stylet was advanced only partially into the brain on the first pass, and removed because the projected sheath/stylet trajectory, based on oblique sagittal and coronal images in the plane of the sheath/stylet, appeared to predict a > 2 mm distance between intended and desired target. In these 3 cases, the sheath/stylet was removed, the alignment stem replaced, a new target alignment was performed with the alignment stem, and the sheath/stylet advanced a second time. The total number of instrument passes into the brain for the 53 DBS lead implants was 60. The maximum number of passes per lead was 2.

Application Accuracy of iMR Imaging DBS

Mean targeting errors in the axial plane at a depth of 4 mm below the commissures (typically corresponding to dorsal STN) are detailed in Table 3. The mean (± SD) radial error for the initial pass of the peel-away sheath/ ceramic stylet assembly was 1.18 ± 0.65 mm. Mean vector errors for lead tip location are shown in Table 4 and compared with previously published reports of STN lead tip errors using traditional frame-based guidance[12,28] (Fig. 9). Mean absolute errors (absolute value of the difference between expected and actual lead tip) and our comparison data from frame-based stereotaxy cases are shown in Table 5. In the x and y dimensions, as well as for the 3D vector error, the errors for iMR imaging–guided DBS were statistically smaller than for frame-based stereotaxy cases. Differences in the z (vertical) plane were not significant. The mean age of patients in the frame-based comparison series was 60.5 years.

Predictors of Lead Placement Accuracy

We checked for possible correlations of target errors with the following potential predictors: case order (reflecting greater experience), patient age, side of surgery, coronal approach angle, and sagittal plane approach angle. The only significant predictor of error was coronal approach angle, with increasing absolute lateral error correlating with increasing (more oblique) coronal approach angle ($r = 0.4$, $p = 0.003$). We did not quantitatively assess cerebral atrophy as a possible predictor of lead placement accuracy. However, cerebral atrophy increases with age, and patient age was not a predictor of accuracy in spite of the wide range of patient ages (44–76 years) in the series.

Clinical Outcomes

Thirteen of the 19 patients who underwent simultaneous bilateral electrode implantation were available for follow-up testing in the off-medication state. At the preoperative baseline, the mean (± SD) UPDRS III score was 49 ± 13 off-medication and 19 ± 8 on-medication. Thus, preoperatively, the patient's usual dose of oral levodopa improved the baseline motor function by 59 ± 15%. At a mean follow-up of 9 months, the mean ± SD UPDRS III score in the on-stimulation and off-medication state was 19 ± 14. Deep brain stimulation produced an improvement in the off-medication state (stimulation on versus baseline) of 60 ± 29%, similar to the preoperative improvement induced by levodopa.

Complications of Implantation

There were no hemorrhages (either symptomatic or asymptomatic) visible on MR images in the 53 implantations. Two hardware infections occurred early in the series, both at the frontal incision (implant nos. 7 and 11), requiring removal of all implanted hardware. One of these was accompanied by cerebritis, requiring a prolonged stay in the intensive care unit, with eventual full recovery. It is notable that both of these occurred prior to the availability of an MR imaging–compatible cranial drill. At that time, the procedure required that the initial exposure and bur hole be made in the room adjacent to the MR imaging unit, followed by a move into the MR imaging bore with partial redraping of the field.[19] Since the introduction of an MR imaging–compatible drill and performance of all parts of the implant in the MR imaging room with a single draping procedure (beginning with the 12th implantation procedure), no further infections associated with the iMR imaging procedure have occurred.

In 1 patient both leads were found to be inadequately placed, based on failure to achieve expected clinical results after multiple programming attempts. In retrospect, this patient had unusual STN anatomy (medially located STNs), a variant that was not fully appreciated on targeting MR imaging, such that the intended target during the iMR imaging procedure did not reflect the actual STN position. Expected clinical benefit was achieved after surgical replacement of the lead to a more medial location (10 mm from midline), using the traditional stereotactic method.

In the comparison group of 76 STN DBS electrodes implanted using traditional frame-based stereotaxy and MR imaging,[28] there were 2 hemorrhages (1 symptomatic and 1 asymptomatic), no hardware infections, and 1 suboptimally placed lead that required surgical repositioning.

Discussion

In the present study, we described our technical approach to iMR imaging–guided DBS placement and measured its application accuracy in 53 STN DBS lead implantations in patients with PD. This technical approach evolved as an extension of the work of Hall and

colleagues[9,10] in high field iMR imaging–guided brain biopsy. They used a smaller "joystick" aiming device (Medtronic Navigus) in their biopsy work, while in the present study we used a skull-mounted device (Medtronic NexFrame) with a "rotate/translate" mechanism; this provided finer control at the expense of a less intuitive aiming paradigm.

Technique Justification

The conceptual basis for the technique rests on prior experience of our group and others with frame-based, microelectrode-guided STN DBS. In general, the criteria for successful STN lead placement have been physiological (region in which microelectrode recording detected STN cells including cells with movement-related responses), or clinical (lead placements that resulted in successful reduction in parkinsonian symptoms). Now 15 years after the introduction of STN DBS,[4] many groups have performed post hoc correlation of lead location by postoperative MR imaging with single-unit physiology,[1,24,25,29] thresholds for stimulation-induced adverse events,[3,27,28] and clinical success.[2,7,16,20,22,23,26,28,30] These authors have shown that the STN can be visualized based on its hyperintensity on T2-weighted MR images, and that the dorsolateral region of the MR imaging–defined STN reliably contains movement-related cells. Brain coordinates predicting clinical success have been elucidated.[2,7,16,20,22,23,26,28,30] This experience provided the conceptual foundation for the use of imaging criteria alone (without physiological studies) to define and confirm the accuracy of target placement. For newer brain targets where correlations of lead location with physiology and outcome are less well understood, the use of imaging alone for lead placement may be less appropriate.

Application Accuracy Superior to Other Approaches

In frame-based and frameless neuronavigation-guided stereotaxy, the application accuracy of the stereotactic method has been calculated as the difference between the expected lead location and the actual location measured on postoperative imaging. To determine the expected lead location, the initial anatomical target coordinates in the AC-PC space are adjusted by intraoperative refinements made by physiological measures. This type of application accuracy measurement reflects a variety of potential errors inherent to stereotaxy, including image distortion, brain shift occurring after imaging but before lead insertion, and the mechanical properties of the frame and guidance system. The vector difference in the expected and actual tip location for both techniques has been reported as 3.2 mm in a recent statistical comparison of frame-based and frameless techniques.[12] We have shown here that the application accuracy of the iMR imaging approach is superior to that in our own initial series of frame-based STN DBS placements,[28] with a 29% improvement in the mean difference between expected and actual tip locations.

The iMR imaging approach, however, may not ultimately result in better final lead placement compared with traditional approaches, because in the latter a relatively inaccurate anatomical placement can be refined (and presumably improved) based on intraoperative physiological or neurological data. The measurement described above reflects the accuracy of the stereotactic approach only, not the final difference between desired and actual coordinates. However, our results do indicate that, when considering the accuracy of the imaging methods and the mechanical guidance platform alone, iMR-guided placement can achieve greater accuracy than the framebased approach alone. Reasons for this superiority may include the integration of imaging and surgery (reducing errors arising from brain shift), the greater simplicity of the guidance platform (compared with frame-based approaches), or the avoidance of registration error between the stereotactic and image space (because these coordinate systems are the same in the iMR imaging approach). Whether this superiority is sufficient to forego physiological refinement with the use of MER (which is impractical in the iMR setting) remains to be justified with clinical outcomes studies. Of

note, iMR offers the possibility of image-based refinement as an alternative to physiological refinement: if the initial lead (or stylet) placement is inadequate based on MR imaging criteria, this can be modified by taking a second pass of the stylet/guidance sheath using real-time imaging.

Error Correlations

We found a significant positive correlation of lateral error with coronal approach angle (measured from the vertical to the AC-PC line). The largest single dimension error in this study, as in traditional techniques, is in the z-axis and may reflect measurement uncertainty in the advancement of the lead along its trajectory. As the approach angle obliquity increases, any error of depth along the trajectory becomes translated into greater error in the horizontal plane. The lack of a similar correlation of anteroposterior error with sagittal approach angle may be because there was relatively less variability in sagittal approach angle (compared with the coronal approach angle) in our series. The relatively oblique coronal approach angle used in this series was designed to avoid transgressing the lateral ventricle because of concern over potential brain deformation induced by oblique contact between the stylet/sheath assembly and the ependymal surface.

Alternative Strategies for Use of Intraoperative MR for DBS Placement

Other approaches to the integration of MR imaging into DBS procedures have been reported. DeSalles and coworkers[17] have investigated the use of intraoperative 0.2-T[6] and 1.5-T imaging using MR imaging devices adapted for the operating room environment. In their approach, leads were placed using traditional frame-based stereotaxy and MER, but the use of intraoperative imaging allowed confirmation of lead position prior to leaving the operating room. In contrast, our technique uses near real-time MR imaging as the sole means of navigation (rather than as a confirmation of traditional navigation) and emphasizes the adaptation of the procedure to diagnostic MR imaging rather than the use of customized intraoperative MR imaging units.

Technical Problems and Future Development

A long-range goal of the iMR imaging approach to DBS implantation is to allow its utilization within any diagnostic MR imaging scanner without making special modifications for surgery. In its current form, however, there are several cumbersome aspects to iMR. First, reaching into the bore of the magnet for manual steering is awkward, especially for those with limited reach. This could be addressed with a mechanical remote control. Secondly, there is some loss of image quality with surface coils compared with rigid “bird cage” coils. Third, the current trajectory guide is not optimized to deal with targeting errors because of limited side channel availability and inability to interpolate smaller distances between the center and side channels. Fourth, the MR console does not have easy turnkey software to perform this procedure, and requires an operator with detailed technical knowledge of the software provided by the MR manufacturer. Moreover, the accuracy of many steps in the procedure relies on the operator’s ability to accurately identify the geometic center of the pivot point and fluid stem. Finally, at this time, the technique requires in-room visualization of the MR fluoroscopy images used to manually perform the stem alignment by the surgeon. Expensive manufacturer-installed in-room monitors could be replaced by a simpler monitor projector setup, as has been described for MR imaging–guided cardiac interventions.[8]

Conclusions

We have developed a technical approach to placement of deep brain stimulators that adapts the procedure to a standard-configuration 1.5-T diagnostic MR imaging scanner in a

radiology suite. The technique uses near realtime MR imaging in conjunction with a skull-mounted aiming device as the sole method of guiding DBS electrodes to the STN and confirming their localization. The accuracy of this method (the difference between expected and actual DBS lead tip locations) was shown to be greater than that of anatomical guidance using standard frame-based stereotaxy and preoperative MR imaging. Our technique may lead to more rapid lead implantation and greater patient comfort than is possible using standard physiologically guided techniques. In patients available for follow-up, the degree of stimulation-induced improvement in the UPDRS III in the off-medication state was 60%, comparable to most studies of STN DBS in which traditional surgical techniques were used. However, clinical outcomes from this technique must be studied in a larger series.

Acknowledgments

The authors thank Lynn Otten of Medtronic, Inc., for providing custom-made titanium wire stylets for the Medtronic model 3389-28 DBS lead, and custom ceramic stylets for the peel-away sheath. Keith Sootsman of Medtronic, Inc., provided technical support for the use of the NexFrame device in the iMR imaging environment. The authors thank Elaine Lanier, Robin Taylor, and Jamie Grace for administrative assistance with preparation of the annual submission of the research protocol to the institutional review board. Monica Volz and William J. Marks Jr. assisted with perioperative patient management and device programming.

Abbreviations used in this paper

AC-PC	anterior commissure–posterior commissure
DBS	deep brain stimulation
iMR	interventional MR
MER	microelectrode recording
PD	Parkinson disease
STN	subthalamic nucleus
UPDRS	Unified Parkinson’s Disease Rating Scale

References

1. Abosch A, Hutchison WD, Saint-Cyr JA, Dostrovsky JO, Lozano AM. Movement-related neurons of the subthalamic nucleus in patients with Parkinson disease. J Neurosurg 2002;97:1167–1172. [PubMed: 12450039]
2. Anheim M, Batir A, Fraix V, Silem M, Chabardes S, Seigneuret E, et al. Improvement in Parkinson disease by subthalamic nucleus stimulation based on electrode placement: effects of reimplantation. Arch Neurol 2008;65:612–616. [PubMed: 18474736]
3. Ashby P, Kim YJ, Kumar R, Lang AE, Lozano AM. Neurophysiological effects of stimulation through electrodes in the human subthalamic nucleus. Brain 1999;122:1919–1931. [PubMed: 10506093]
4. Benabid AL, Pollak P, Gross C, Hoffman D, Benazzouz A, Gao DM, et al. Acute and long-term effects of subthalamic nucleus stimulation in Parkinson’s disease. Stereotact Funct Neurosurg 1994;62:76–84. [PubMed: 7631092]
5. Black PM, Alexander E, Martin C, Moriarty T, Nabavi A, Wong TZ, et al. Craniotomy for tumor treatment in an intraoperative magnetic resonance imaging unit. Neurosurgery 1999;45:423–433. [PubMed: 10493363]
6. De Salles AA, Frighetto L, Behnke E, Sinha S, Tseng L, Torres R, et al. Functional neurosurgery in the MRI environment. Minim Invasive Neurosurg 2004;47:284–289. [PubMed: 15578341]
7. Godinho F, Thobois S, Magnin M, Guenot M, Polo G, Benatru I, et al. Subthalamic nucleus stimulation in Parkinson’s disease: anatomical and electrophysiological localization of active contacts. J Neurol 2006;253:1347–1355. [PubMed: 16788774]

8. Guttman MA, Ozturk C, Raval AN, Raman VK, Dick AJ, De-Silva R, et al. Interventional cardiovascular procedures guided by real-time MR imaging: an interactive interface using multiple slices, adaptive projection modes and live 3D renderings. J Magn Reson Imaging 2007;26:1429–1435. [PubMed: 17968897]
9. Hall WA, Liu H, Martin AJ, Maxwell RE, Truwit CL. Brain biopsy sampling by using prospective stereotaxis and a trajectory guide. J Neurosurg 2001;94:67–71. [PubMed: 11147900]
10. Hall WA, Martin AJ, Liu H, Nussbaum ES, Maxwell RE, Truwit CL. Brain biopsy using high-field strength intervention-al magnetic resonance imaging. Neurosurgery 1999;44:807–814. [PubMed: 10201306]
11. Henderson JM, Holloway KL, Gaede SE, Rosenow JM. The application accuracy of a skull-mounted trajectory guide system for image-guided functional neurosurgery. Comput Aided Surg 2004;9:155–160. [PubMed: 16192055]
12. Holloway KL, Gaede S, Starr PA, Rosenow J, Ramakrishnan V, Henderson J. Frameless stereotaxy using bone fiducials for deep brain stimulation. J Neurosurg 2005;103:404–413. [PubMed: 16235670]
13. Jolesz FA. Future perspectives for intraoperative MRI. Neurosurg Clin N Am 2005;16:201–213. [PubMed: 15561539]
14. Kanner AA, Vogelbaum MA, Mayberg MR, Weisenberger JP, Barnett GH. Intracranial navigation by using low-field intraoperative magnetic resonance imaging: preliminary experience. J Neurosurg 2002;97:1115–1124. [PubMed: 12450034]
15. Lang AE, Houeto JL, Krack P, Kubu C, Lyons KE, Moro E, et al. Deep brain stimulation: preoperative issues. Mov Disord 2006;21 (14 Suppl):S171–S196. [PubMed: 16810718]
16. Lanotte MM, Rizzone M, Bergamasco B, Faccani G, Melcarne A, Lopiano L. Deep brain stimulation of the subthalamic nucleus: anatomical, neurophysiological, and outcome correlations with the effects of stimulation. J Neurol Neurosurg Psychiatry 2002;72:53–58. [PubMed: 11784826]
17. Lee MW, De Salles AA, Frighetto L, Torres R, Behnke E, Bronstein JM. Deep brain stimulation in intraoperative MRI environment—comparison of imaging techniques and electrode fixation methods. Minim Invasive Neurosurg 2005;48:1–6. [PubMed: 15747209]
18. Maciunas RJ, Galloway RL, Latimer JW. The application accuracy of stereotactic frames. Neurosurgery 1994;35:682–695. [PubMed: 7808612]
19. Martin AJ, Larson P, Ostrem J, Sootsman K, Weber O, Lindsey N, et al. Placement of deep brain stimulator electrodes using real-time high field interventional MRI. Magn Reson Med 2005;54:1107–1114. [PubMed: 16206144]
20. McClelland S III, Ford B, Senatus PB, Winfield LM, Du YE, Pullman SL, et al. Subthalamic stimulation for Parkinson disease: determination of electrode location necessary for clinical efficacy. Neurosurg Focus 2005;19(5):E12. [PubMed: 16398462]
21. Moriarty TM, Quinones-Hinojosa A, Larson PS, Alexander E III, Gleason PL, Schwartz RB, et al. Frameless stereotactic neurosurgery using intraoperative magnetic resonance imaging: stereotactic brain biopsy. Neurosurgery 2000;47:1138–1146. [PubMed: 11063107]
22. Okun MS, Tagliati M, Pourfar M, Fernandez HH, Rodriguez RL, Alterman RL, et al. Management of referred deep brain stimulation failures: a retrospective analysis from 2 movement disorders centers. Arch Neurol 2005;62:1250–1255. [PubMed: 15956104]
23. Plaha P, Ben-Shlomo Y, Patel NK, Gill SS. Stimulation of the caudal zona incerta is superior to stimulation of the subthalamic nucleus in improving contralateral parkinsonism. Brain 2006;129:1732–1747. [PubMed: 16720681]
24. Rodriguez-Oroz MC, Rodriguez M, Guridi J, Mewes K, Chockkman V, Vitek J, et al. The subthalamic nucleus in Parkinson's disease: somatotopic organization and physiological characteristics. Brain 2001;124:1777–1790. [PubMed: 11522580]
25. Romanelli P, Heit G, Hill BC, Kraus A, Hastie T, Bronte-Stewart HM. Microelectrode recording revealing a somatotopic body map in the subthalamic nucleus in humans with Parkinson disease. J Neurosurg 2004;100:611–618. [PubMed: 15070113]

26. Saint-Cyr JA, Hoque T, Pereira LCM, Dostrovsky JO, Hutchison WD, Mikulis DJ, et al. Localization of clinically effective stimulating electrodes in the human subthalamic nucleus on magnetic resonance imaging. J Neurosurg 2002;97:1152–1166. [PubMed: 12450038]

27. Shields DC, Gorgulho A, Behnke E, Malkasian D, DeSalles AA. Contralateral conjugate eye deviation during deep brain stimulation of the subthalamic nucleus. J Neurosurg 2007;107:37–42. [PubMed: 17639871]

28. Starr PA, Christine C, Theodosopoulos PV, Mosely T, Byrd D, Lindsey N, et al. Implantation of deep brain stimulator electrodes into the subthalamic nucleus: technical approach and magnetic resonance imaging-verified electrode locations. J Neurosurg 2002;97:370–387. [PubMed: 12186466]

29. Theodosopoulos PV, Marks WJ, Christine C, Starr PA. The locations of movement-related cells in the human Parkinsonian subthalamic nucleus. Mov Disord 2003;18:791–798. [PubMed: 12815658]

30. Zonenshayn M, Sterio D, Kelly PJ, Rezai AR, Beric A. Location of the active contact within the subthalamic nucleus (STN) in the treatment of idiopathic Parkinson's disease. Surg Neurol 2004;62:216–226. [PubMed: 15336862]

Fig. 1.
Intraoperative photograph showing the position of the patient's head in an MR-compatible headholder with placement of radiofrequency surface coils. The connection between the endotracheal tube and ventilator is led through the anterior coil. The posterior coil, placed under the headholder, is hidden under a towel.

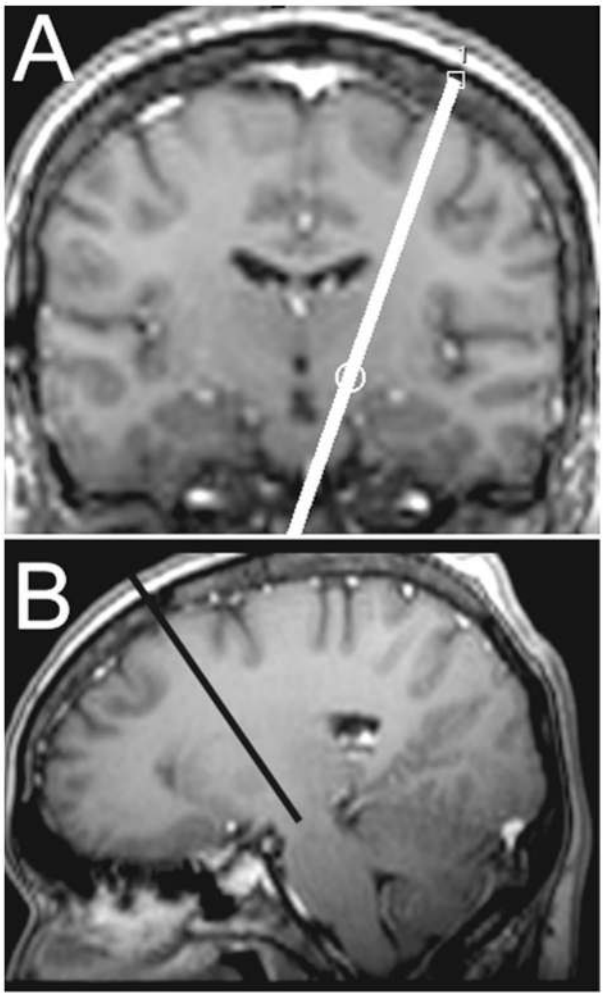

Fig. 2.

Magnetic resonance images showing the method of trajectory planning using reformatted oblique slices passing through the target, angled to exclude the lateral ventricle (MR protocol 1). **A:** First step. On a coronal plane passing through the target, an oblique sagittal plane is defined *(white line)* that avoids the lateral ventricle. **B:** Second step. The oblique sagittal plane selected in panel A is constructed on the MR console, and a safe trajectory *(black line)* to the target is planned.

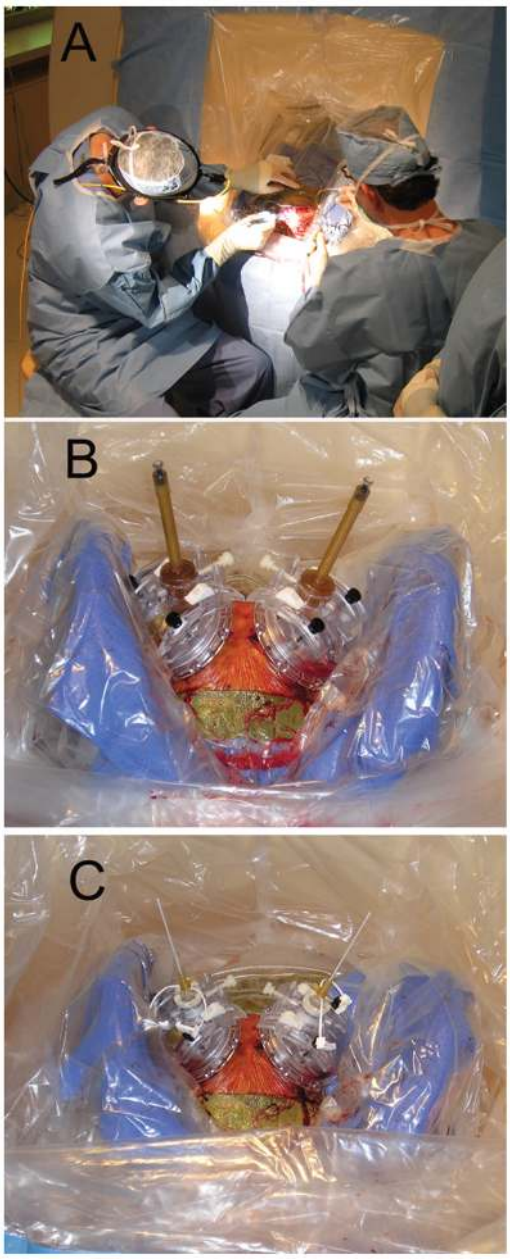

Fig. 3.

Intraoperative photographs demonstrating surgical draping and trajectory guides. **A:** Patient's head is shown at the back of the MR bore, with a sterile drape. **B:** Trajectory guides with alignment stems are shown. **C:** Trajectory guides with multilumen insert and peel-away sheath prior to advancing the sheath into the brain. The flexible radiofrequency receiving coils are covered with sterile blue towels.

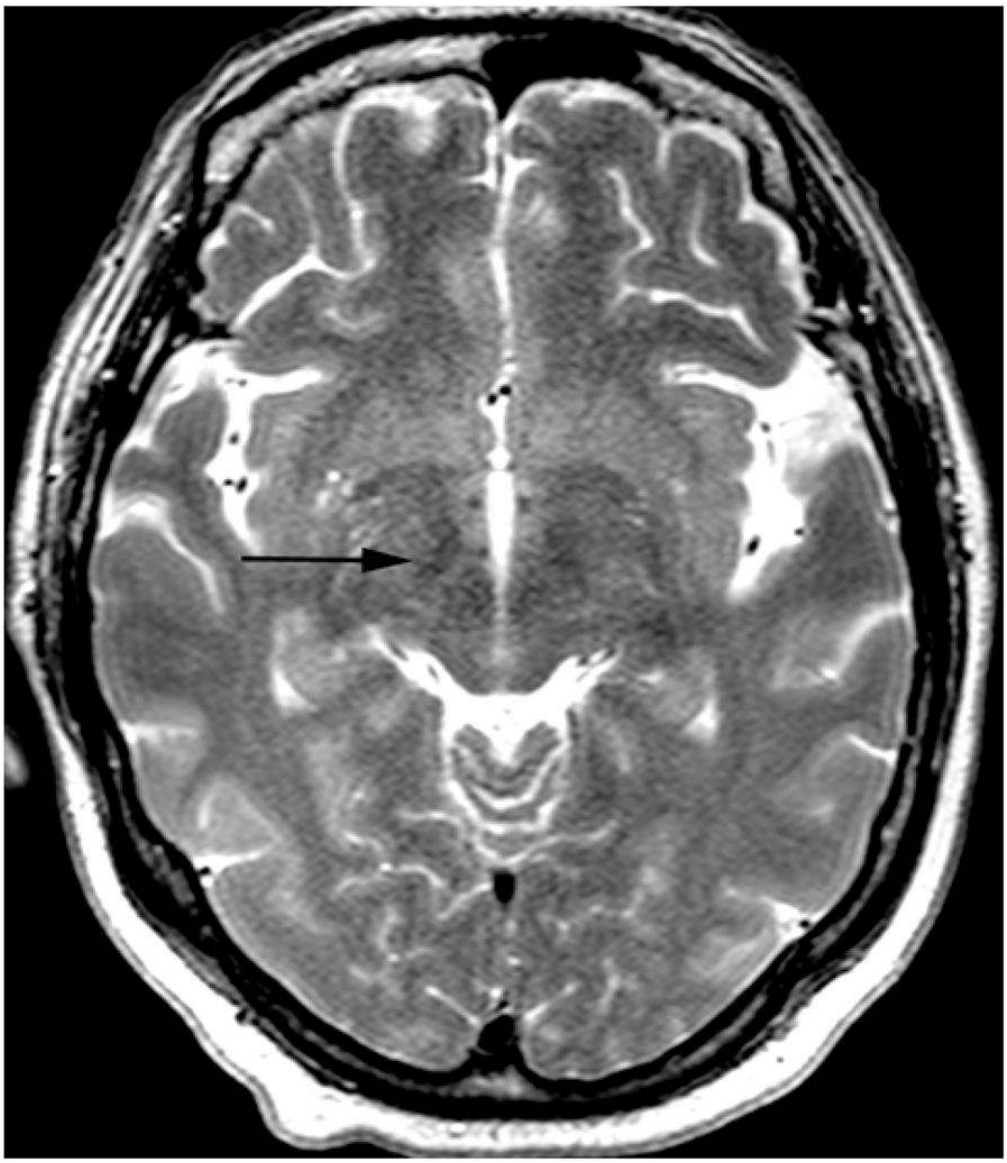

Fig. 4.
Axial MR image used to define the target in the dorsolateral STN (*black arrow* indicates right STN; MR protocol 3).

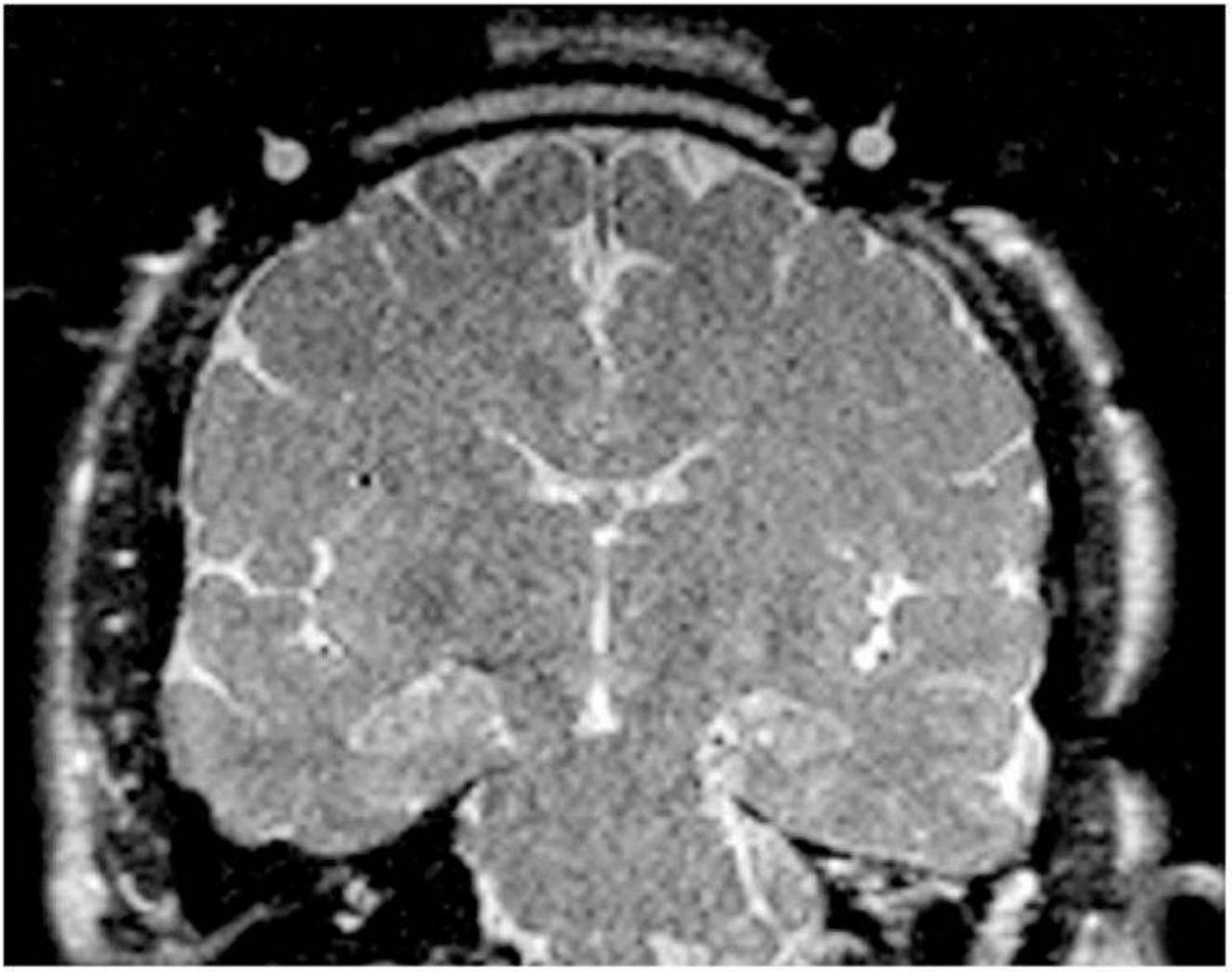

Fig. 5.
Coronal MR image used to define the coordinates of the pivot points for the trajectory guides, prior to aligning the alignment stem (MR protocol 4).

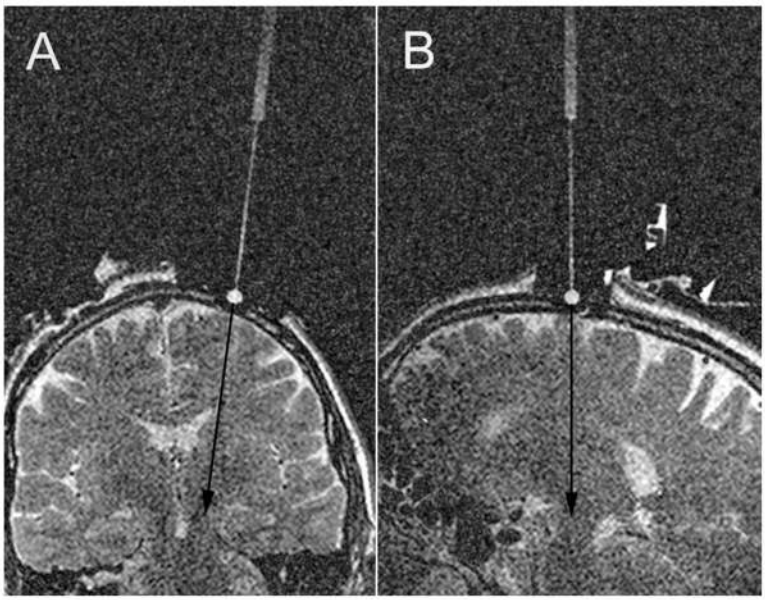

Fig. 6.

Rapid acquisition oblique coronal **(A)** and sagittal **(B)** images passing through the target and pivot point after the trajectory guide has been aligned (MR protocol 5). *Black arrows* show the predicted trajectory of the DBS lead.

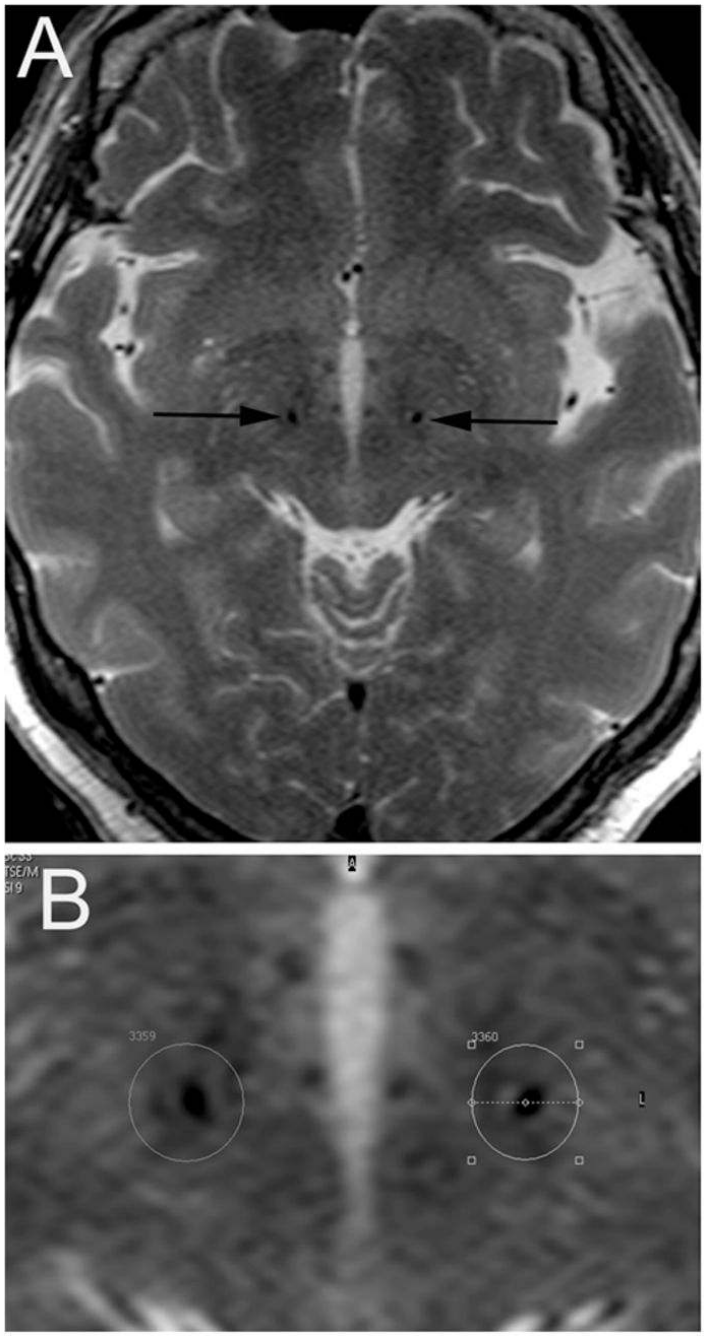

Fig. 7.

A and B: Axial T2-weighted MR images obtained 4 mm below the commissures, showing sheath and ceramic stylet assembly at target (MR protocol 3). Close up **(B)** showing the stylets in the target region, with the desired targets indicated by the centers of the *white circles*. The right lead has a radial error of 0.5 mm in the medial direction. The left lead has a radial error of 0.2 mm in the lateral direction.

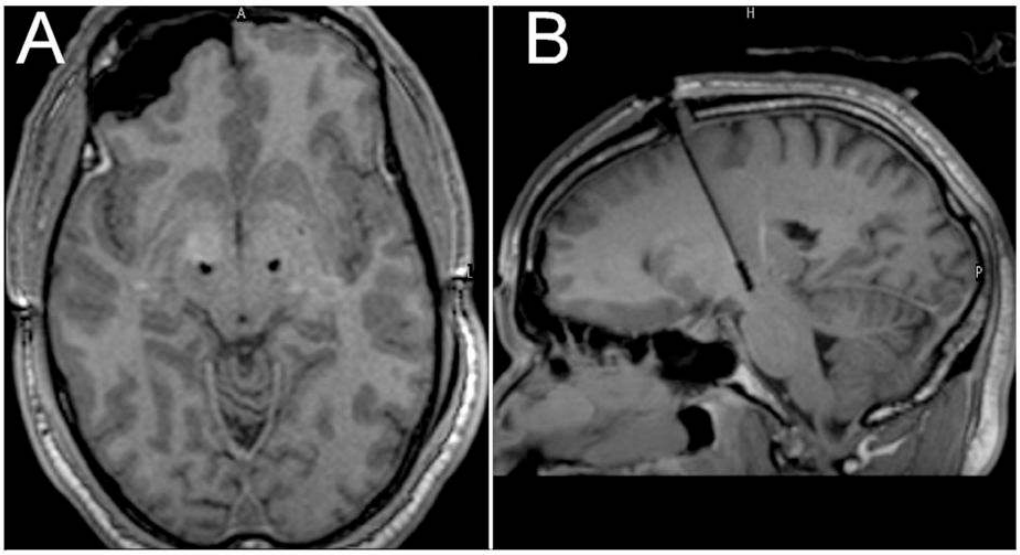

Fig. 8.

Final lead location as assessed on T1-weighted volumetric MR images. **A:** Axial image at 4 mm inferior to the commissures. **B:** Reformatted oblique image in the sagittal plane along the lead trajectory (MR protocol 8).

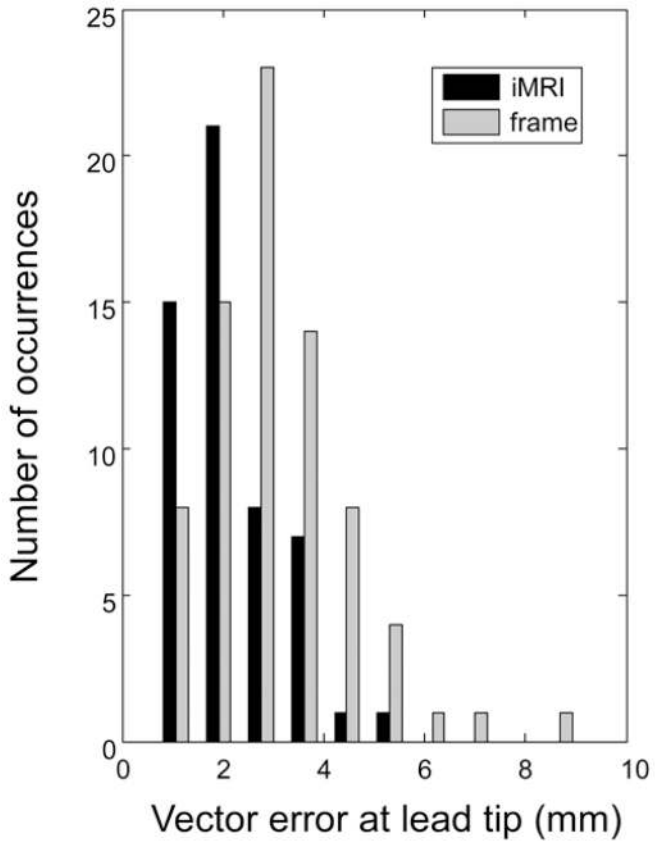

Fig. 9.

Bar graph showing the distribution of lead tip errors (3D or vector error) in STN DBS placed using iMR imaging versus frame-based stereotaxy. Comparison data are from Starr et al., 2002.

TABLE 1

Equipment used for iMR imaging–guided DBS*

Item	Manufacturer	Description/Use
Intera 1.5-T intraoperative MRI	Philips Medical Systems	bore dimensions: length 157 cm, diameter 60 cm; used for routine diagnostic imaging & interventional procedures
Malcolm Rand headset	Integra Life Sciences	MRI-compatible carbon fiber headholder
Stimloc cranial base & cap	Medtronic, Inc.	for long-term cranial fixation of permanent electrodes; currently used at UCSF for most DBS lead implant procedures
NexFrame trajectory guide & alignment stem	Medtronic, Inc.	disposable skull-mounted aiming device
NexFrame Peel-Away Introducer	Medtronic, Inc.	standard peel-away introducer design intended for use in conjunction w/the NexFrame family of trajectory guides to deliver devices into the brain
ceramic stylet for NexFrame Peel-Away Introducer	Medtronic, Inc.	nonmetallic rigid stylet, fits inner diameter of peel-away introducer, for inserting introducer into brain
model 3389 28-cm DBS electrode	Medtronic, Inc.	one of a family of DBS electrodes currently used for DBS implantation procedures; length (28 cm) is shorter than in standard frame-based procedures
Ti stylet for DBS electrode	Medtronic, Inc.	custom MR-compatible stylet associated w/relatively low MR artifact
gas-powered MRI compatible cranial drill	Anspach, Inc.	nitrogen tank used to power the drill is not MRI-compatible & is kept outside of the MRI room
Ti surgical instruments	KMedic Instruments	set includes: Adson forceps, Metzenbaum scissors, Mayo scissors, 3-mm Kerrison rongeur, Penfield dissectors, Debakey forceps, hemostats, & needle holder

* UCSF = University of California, San Francisco.

TABLE 2

Magnetic resonance imaging pulse sequences for iMR imaging–guided DBS*

Protocol No.	**1**	**2**	**3**	**4**	**5**	**6**	**7**	**8**
protocol description	IR volumetric T1W 3D GE	MR fluoroscopy sequence	HR axial T2W FSE	volumetric 3D T2W FSE	LR T2W FSE	HR T2W FSE	IR T2W FSE	HR volumetric T1W 3D GE
purpose	trajectory planning	marking scalp entry point, alignment of the fluid-filled stem	identification of STN target point, confirmation of stylet position	identification of the alignment stem pivot points	confirmation of trajectory of alignment stem	confirmation of trajectory of stylet during brain entry	confirmation of lead depth	postplacement lead location measurements
acquisition plane	axial	oblique axial	axial	coronal & sagittal	oblique coronal & sagittal	oblique coronal & sagittal	axial	axial
slice thickness (mm)	2.0	1.2	2.0	1.0	2.0	1.0	1.0	1.5
FOV (mm)	260 × 207	128 × 104	260 × 222	256 × 256	250 × 188	256 × 216	256 × 192	260 × 222
no. of slices	75	1	21	9	3	11	15	120
TR	20	5.5	3000	2000	2000	2000	3000	20
TE	2.9	2.8	90	100	103	96	90	3.2
matrix size	176 × 114	128 × 103	384 × 224	256 × 256	256 × 192	256 × 172	256 × 192	192 × 152
flip angle (°)	30	60	90	90	90	90	90	30
NEX	1	1	6	1	1	1	1	1
echo train length	NA	NA	16	54	24	56	42	NA
bandwidth (kHz)	54	75	40	182	115	160	88	50
SAR (W/kg)	0.3	0.9	1.0	0.8	1.2	1.0	0.5	0.3
scan time (minutes:seconds)	4:09	5 frame/sec†	8:42	1:28	0:18	1:22	4:06	8:54

*FOV = field of view; FSE = fast spin echo; GE = gradient echo; HR = high resolution; IR = intermediate resolution; LR = low resolution; NA = not applicable; NEX = number of excitations; SAR = specific absorption rate; T1W = T1-weighted; T2W = T2-weighted.

†Each scan duration was 600 msec, but they were stacked so as to present at 5 frames/sec.

TABLE 3

Difference between expected and actual lead (or stylet) locations (in mm) for iMR imaging–guided STN DBS (53 leads)*

Lateral (X)	AP (Y)	|X|	|Y|	Vector Error $(X^2 + Y^2)^{1/2}$	Radial Error for Stylet
−0.58 ± 0.86	−1.21 ± 1.01	0.80 ± 0.65	1.30 ± 0.88	1.65 ± 0.90	1.18 ± 0.65

*All columns refer to final lead measurements except for radial error, which refers to the difference between expected and actual location of the first insertion of the stylet/peel-away sheath assembly prior to lead insertion.

Positive values for X and Y signify lateral and anterior directions, respectively. Results are given as means ± SDs. Abbreviation: AP = anteroposterior.

TABLE 4

Targeting errors in millimeters for the lead tip (difference between expected and actual lead tip locations), for iMR imaging compared with literature data on Leksell frame-based DBS (76 leads)*

Technique	X Error	Y Error	Z Error	Vector $(X^2 + Y^2 + Z^2)^{1/2}$
iMRI	−0.07 ± 0.96	0.15 ± 1.10	1.36 ± 1.27	2.18 ± 0.92
frame-based stereotaxy	−0.76 ± 1.48	0.57 ± 1.73	0.86 ± 2.14	3.06 ± 1.41
p value for difference between iMRI & frame-based errors	0.004†	0.009†	0.129	0.0001†

*Data are presented as means ± SDs.

Positive values for x, y, and z signify lateral, anterior, and superior directions, respectively. Frame-based stereotaxy data derived from Starr et al., 2002.

†Statistically significant difference in 2-sample unpaired t-test for equality of means at $p < 0.05$.

TABLE 5

Summary of absolute targeting errors measured at the lead tip (difference between expected and actual lead tip locations in mm) for iMR imaging–guided STN DBS versus Leksell frame-based stereotaxy (in 76 leads)

Group	|X|	|Y|	|Z|
iMRI	0.73 ± 0.62	0.85 ± 0.70	1.54 ± 1.05
frame-based stereotaxy*	1.36 ± 0.94	1.46 ± 1.09	1.80 ± 1.44
p value for difference btwn iMRI & frame-based accuracy	0.00004†	0.0004†	0.27

*Data from Starr et al., 2002.

†Statistically significant difference in 2-sample unpaired t-test for equality of means at $p < 0.05$. Values are given as means ± SDs.